Biochemical Pharmacology, Vol. 57, pp. 753–762, 1999.

ISSN 0006-2952/99/$–see front matter
PII S006-2952(98)00345-1

Cytokinetics of a Novel 1,2,3-Triazene-Containing Heterocycle, 8-Nitro-3-methyl-benzo-1,2,3,5-tetrazepin-4(3*H*)-one (NIME), in the Human Epithelial Ovarian Cancer Cell Line OVCAR-3

Bertrand Jacques Jean-Claude,† Amir Mustafa,* Zoe Damian,* Josie De Marte,* Daniela Eliza Vasilescu,* Rose Yen,‡ Thak Hang Chan‡ and Brian Leyland-Jones**

Departments of *Oncology and ‡Chemistry, McGill University, Montreal, Quebec, Canada

ABSTRACT. The mechanism of action of the novel tetrazepinone 8-nitro-3-methyl-benzo-1,2,3,5-tetrazepin-4(3*H*)-one (NIME), structurally related to the antitumour drug temozolomide, was studied in the human ovarian tumour cell line OVCAR-3. NIME preferentially inhibited DNA synthesis over protein and RNA syntheses at 3 and 24 hr post-treatment. A Maxam-Gilbert sequencing assay showed that NIME induced barely detectable levels of guanine N^7 alkylation in an isolated DNA strand, in contrast to temozolomide, a strong alkylating agent containing, like NIME, a cyclic 3-methyl-1,2,3-triazene moiety. Alkaline sucrose density-gradient sedimentation, at concentrations 2- to 10-fold lower than the ones used in the DNA sequencing assay, showed significant DNA damage in OVCAR-3 cells 24 hr after treatment with NIME. This was accompanied by a significant accumulation of cells in late S and G_2M. Cell cycle arrest was transient and was reversed after 2–3 days following drug treatment. This was in agreement with bivariate bromodeoxyuridine/propidium iodide analysis, which showed that at 100 μM, a concentration at which the majority of the cells arrested in late S and G_2M, a significant fraction of bromodeoxyuridine positive (S-phase) cells escaped the block. In an attempt to elucidate the mechanism underlying these effects, the degradation of NIME in cell culture medium was analyzed by GC–MS (gas chromatography coupled with mass spectrometry). The results showed that, in contrast to temozolomide, NIME did not convert to an open-chain alkyltriazene in cell culture medium, but to a major benzimidazole product, which exerted a minor effect on the cell cycle. This suggests that NIME, despite containing a 3-(alkyl)-1,2,3-triazene moiety, does not act by DNA alkylation but probably by generating a short-lived genotoxic species during its degradation to 6,5-benzofused derivatives. BIOCHEM PHARMACOL **57**;7: 753–762, 1999. © 1999 Elsevier Science Inc.

KEY WORDS. tetrazepinones; temozolomide; cell cycle arrest; OVCAR-3 cells

BCNU§ and CCNU have established antitumor activity against human brain tumours and lymphomas [1–3]. The simultaneous development of the alkyltriazene class gave rise to Dacarbazine [DTIC; 5-(3,3-dimethyl-1-triazenyl)imidazole-4-carboxamide], which is used in the treatment of Hodgkin's disease and malignant melanoma [1, 4]. Dacarbazine requires metabolic oxidation in order to generate a monomethyltriazene of type **3** (Scheme 1), the putative cytotoxic metabolite [5–8]. However, metabolic oxidation decreases the plasma level of this drug and consequently reduces its activity. In the past decade, the search for stable prodrugs of the Dacarbazine-derived monomethyltriazene has led to the development of the imidazotetrazinone class, which in turn has given rise to two potential antitumour drugs: temozolomide (**1a**) and mitozolomide (**1b**) (Scheme 1) [9]. Unlike Dacarbazine, which requires metabolic activation, these drugs are capable of generating the cytotoxic monoalkyltriazene species **3** under mild alkaline conditions as depicted in Scheme 1 [10]. Following preclinical studies, both mitozolomide and temozolomide underwent Phase I clinical testing [11, 12]. Mitozolomide showed severe thrombocytopenia, which was thought to be associated with its cross-linking ability, and development of the drug was discontinued [11]. In contrast, temozolomide has demonstrated Phase II activity against malignant melanoma, high-grade glioma, and mycosis fungoides [13]. Despite this level of clinical activity, temozolomide is unfortunately inactive against Mer^+ alkylating-agent-resistant cell lines [14–16]. This resistance has been correlated with the expression of high levels of O^6-alkylguanine DNA methyl transferase (MGMT), an enzyme

† Corresponding author: Bertrand Jacques Jean-Claude, Ph.D., Department of Oncology, McGill University, McIntyre Medical Building, Room 701, 3655 Drummond Street, Montreal, Quebec, Canada H3G 1Y6. Tel. (514) 398-8986; FAX (514) 398-5353.

§ *Abbreviations*: BCNU, 1,3-bis-(2-chloroethyl)-1-nitrosourea; BrdUrd, (+)-5-bromo-2′-deoxyuridine; CCNU, 1-chloroethyl-2-cyclohexyl-1-nitrosourea; FITC, fluorescein isothiocyanate, isomer I; NIME, 8-nitro-3-methyl-benzo-1,2,3,5-tetrazepin-4(3*H*)-one; and PI, propidium iodide.

Received 7 January 1998; accepted 8 September 1998.

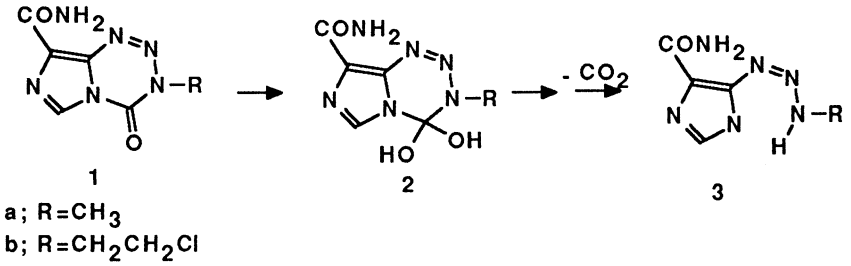

SCHEME 1

capable of repairing the temozolomide-induced O^6-alkylguanine DNA lesions [14].

The limitations of this very promising imidazotetrazinone class of drugs stimulated our interest in designing and synthesizing novel antitumour heterocycles with an improved therapeutic index. In the past 3 years, we have developed a novel ring system containing the basic features of temozolomide and mitozolomide: the 1,2,3,5-tetrazepin-4-ones of type **4** (see Scheme 2) containing the *N*,*N*-alkyl and ureido moieties [17–21].

In contrast to the tetr**azi**nones, the new tetr**azepi**nones show great structural variability. They can be formulated as both bi- and tricyclic systems. In *in vitro* testing, the tetrazepinones show significant antiproliferative activity against a variety of human tumour cell lines including MGMT-proficient brain, breast, and colon tumour cells [22]. In this study, we describe several characteristics of one of our novel tetrazepinones, NIME (**4**), in OVCAR-3 cells. This cell line was one of the most sensitive to NIME in our screening panel. The results suggest that NIME may induce cytotoxicity by a mechanism significantly different from that of temozolomide and related alkylating agents.

MATERIALS AND METHODS

Drug Treatment

NIME was synthesized in our laboratories [17, 23]. In all assays, the drug was dissolved in DMSO and diluted in sterile RPMI medium immediately before treatment of cell cultures. The concentration of DMSO never exceeded 1% (v/v). Cells were either (a) treated with NIME for 2 hr; treatments were terminated by aspiration of the drug-containing medium and replacement with fresh RPMI-1640 medium, or (b) under continuous exposure, where the cells were kept in contact with the drug for the specified time periods.

Cell Culture

The OVCAR-3 cell line [24], obtained from the National Cancer Institute, was maintained as a monolayer culture at 37° in a humidified atmosphere of 5% CO_2–95% air in RPMI-1640 supplemented with fetal bovine serum (10%), L-glutamine (2 mM), penicillin (50 U/mL), and streptomycin (50 mg/mL). Cells were maintained in logarithmic growth by harvesting with a trypsin-EDTA solution containing 0.5 mg/mL of trypsin and 0.2 mg/mL of EDTA and replating before confluency. Growth studies showed a doubling time of approximately 30 hr. In all assays, the cells were plated for 24 hr prior to drug administration.

Clonogenic Assay

Single cell suspensions of 50,000 cells in RPMI medium supplemented with 10% fetal bovine serum were plated in

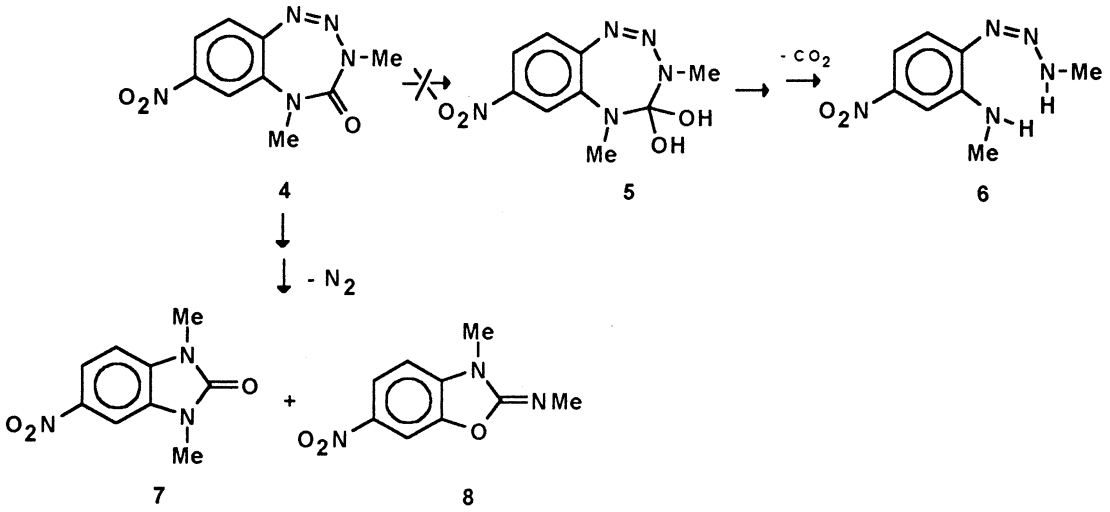

SCHEME 2

25-cm^2 canted-neck Corning flasks. Cells were plated at a density that yielded approximately 1500 colonies/flask in untreated controls. NIME cytotoxicity was assayed by a 2-hr exposure to the drug, followed by recovery of OVCAR-3 cells in drug-free medium. Following incubation of the plated cells under routine conditions for 7 days, colonies were counted with an Artek Omnicon 880 counter, by which time colonies greater than 60 μm were enumerated. Between experiments, percent clonogenic survival was determined as the mean number of colonies from duplicate platings at each drug concentration relative to untreated controls.

Growth Inhibition Kinetics

Cell monolayers were incubated with various amounts of NIME for different time periods, and cytotoxicity was evaluated by the sulforhodamine B assay [25]. Briefly, at each time point, the cells were fixed by the addition of 50 μL of cold trichloroacetic acid (TCA) (50%) at 4° for 60 min. The wells were washed four times with water and stained with sulforhodamine B (0.4%) dissolved in 1% acetic acid. The plates were air-dried, and the resulting colored residue was dissolved in 200 μL of Tris base (10 mM). The optical density of each well was measured at 540 nm with a Bio-Rad microplate reader (model 3550). Points represent the average of two independent experiments run in triplicate.

Degradation

NIME (2 mg) was dissolved in DMSO (20 μL), and the resulting solution was added to cell culture medium (3 mL). The mixture was kept at 37° for 24 hr, after which the water was evaporated *in vacuo*. The resulting residue was reconstituted in methanol (200 μL), and analyses were performed with a Varian 3400 GC equipped with a Finnigan A 200S GC autosampler operating in a splitless mode. A Finnigan MAT model Incos 50 mass spectrometer (Finnigan Nat. Corp.) was used.

NIME was dissolved in DMSO, serially diluted with culture medium in 10 mL tubes, and kept in an incubator at 37°. At each time point (0–24 hr), 200 μL was taken and administered to cells previously allowed to attach to a 96-well plate. Cytotoxicity was determined by the sulforhodamine B assay after 3 days.

Macromolecule Synthesis

DNA, RNA, and protein syntheses were determined by adding the radioactive precursors [*methyl*-^{3}H]thymidine (sp. act. 20 mCi/mmol), [5-^{3}H]uridine (sp. act. 20 mCi/mmol), or L-[4,5-^{3}H]leucine (sp. act. 120–190 Ci/mmol) to the cell culture medium for 3 hr. [*methyl*-^{3}H]Thymidine and [5-^{3}H]uridine (obtained from New England Nuclear) were added at 0.5 μCi/mL, and L-[4,5-^{3}H]leucine (New England Nuclear) at 1 μCi/mL. At the end of radioisotope incubation, cells were trypsinized, and an aliquot (0.1 mL) was collected for cell counts in a ZM Coulter counter before centrifugation. The supernatant was removed and replaced with cold 10% TCA (1 mL). The resulting precipitate was collected by centrifugation and digested in NaOH (0.1 N). The mixture was neutralized, transferred to a scintillation vial, and dissolved in 3 mL of liquid scintillation fluid (Universol). The associated radioactivity was counted in a beta scintillation spectrometer. The level of incorporation was expressed as counts per minute per cell and the percent of control calculated as counts per minute per 10^5 cells

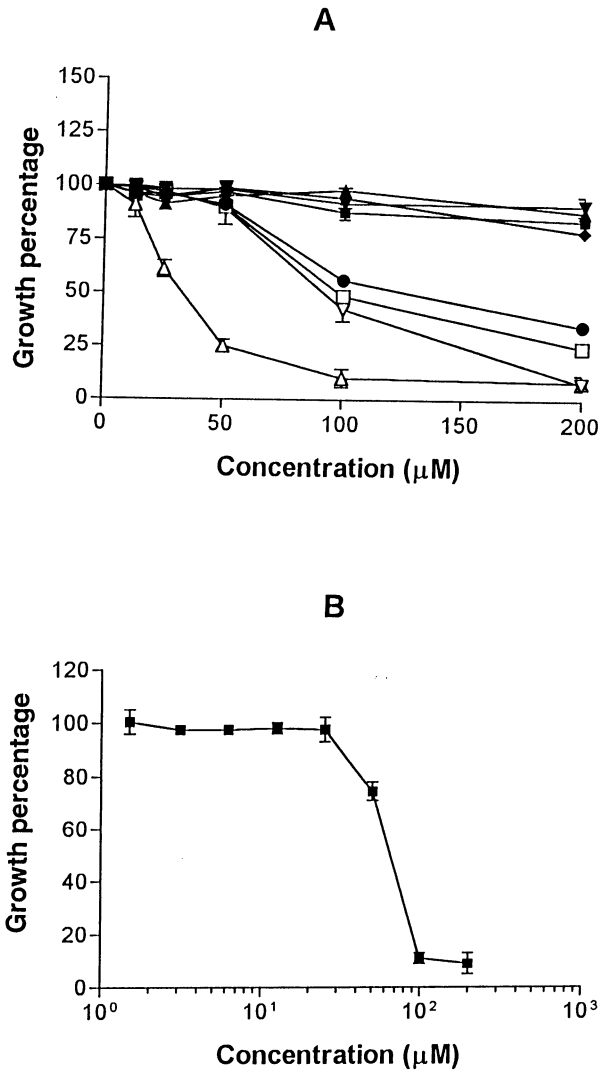

FIG. 1. (A) Growth inhibition kinetics by NIME as determined by the sulforhodamine B assay. OVCAR-3 cells plated at a density of approximately 875 cells/mL were treated for 2 hr with drug and then incubated in drug-free culture medium for various amounts of time: 3 hr (■), 6 hr (▲), 12 hr (▼), 24 hr (♦), 48 hr (●), 72 hr (□), 120 hr (▽), and 168 hr (△). Points in A and B represent means ± SD obtained from two separate experiments run in triplicate, and IC_{50} values were determined by a sigmoidal concentration–response curve fit (variable slope). (B) Survival of clonogenic cells plated at a density of 6 × 10^5 cells/mL from the OVCAR-3 cell line after *in vitro* exposure for 2 hr to increasing concentrations of NIME. Colonies were counted 7 days after treatment.

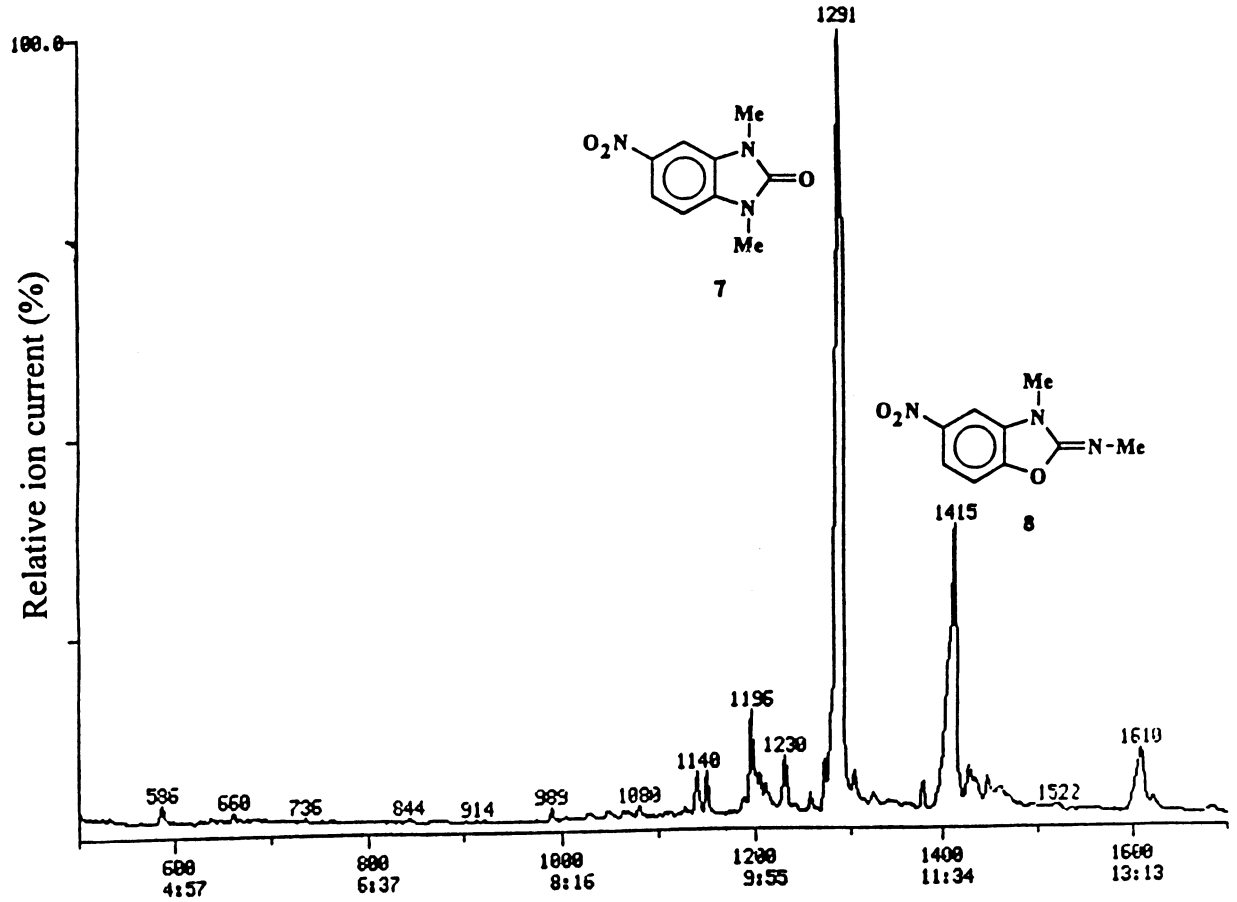

FIG. 2. Identification of metabolites resulting from the degradation of NIME in cell culture medium. The gas chromatogram shows the formation of a major metabolite (peak #1291) with mass spectrum corresponding to 7, and a minor metabolite (peak #1415), which was assigned structure 8, based on mass spectrometric analysis.

treated divided by counts per minute per 10^5 control cells. Each point represents the mean and standard deviation resulting from at least two independent experiments run in duplicate.

Flow Cytometry

SINGLE PARAMETER. The effects of a 2-hr exposure to NIME and its metabolite **7** (see Scheme 2) on the cycle of OVCAR-3 cells were evaluated after recovery times of 24, 48, 72, 96, and 120 hr. The cells were harvested by trypsinization at the appropriate times. After fixation in ethanol (70%, v/v), they were stained with an aqueous PI solution (100 μg/mL) containing RNase (50 μg/mL) for 30 min at 37° in the dark. The fluorescence was detected in a spectral range between 580 and 750 nm. Each cytometric analysis was performed on a Becton Dickinson FACScan instrument on 1–3 × 10^5 cells. The percentage of cells in each cell cycle phase was estimated using LYSYS II software (Becton Dickinson).

BIVARIATE BRDURD/PI ANALYSIS. To examine the fate of S-phase cells, a bivariate BrdUrd/PI flow cytometric technique was used [18, 26, 27]. After a 2-hr drug exposure, the cells were pulse-labeled for 30 min with BrdUrd (10 μM), and the analyses were performed at specified time points. The cells were fixed in ethanol (70%), pelleted by centrifugation, washed with PBS, resuspended in 1 mL of

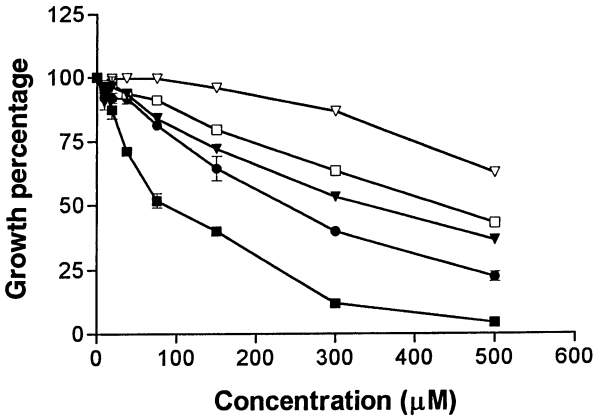

FIG. 3. Growth inhibitory activity of NIME after different preincubation times of the drug in cell culture medium for various times at 37°: 0 hr (■), 0.25 hr (●), 0.5 hr (▼), 14 hr (□), and 24 hr (▽). Growth percentage was evaluated after 72 hr by the sulforhodamine B assay in OVCAR-3 cells plated at a density of approximately 1000 cells/mL. Increase in growth percentage corresponds to decrease in drug activity. Data are means ± SD of two separate experiments run in triplicate.

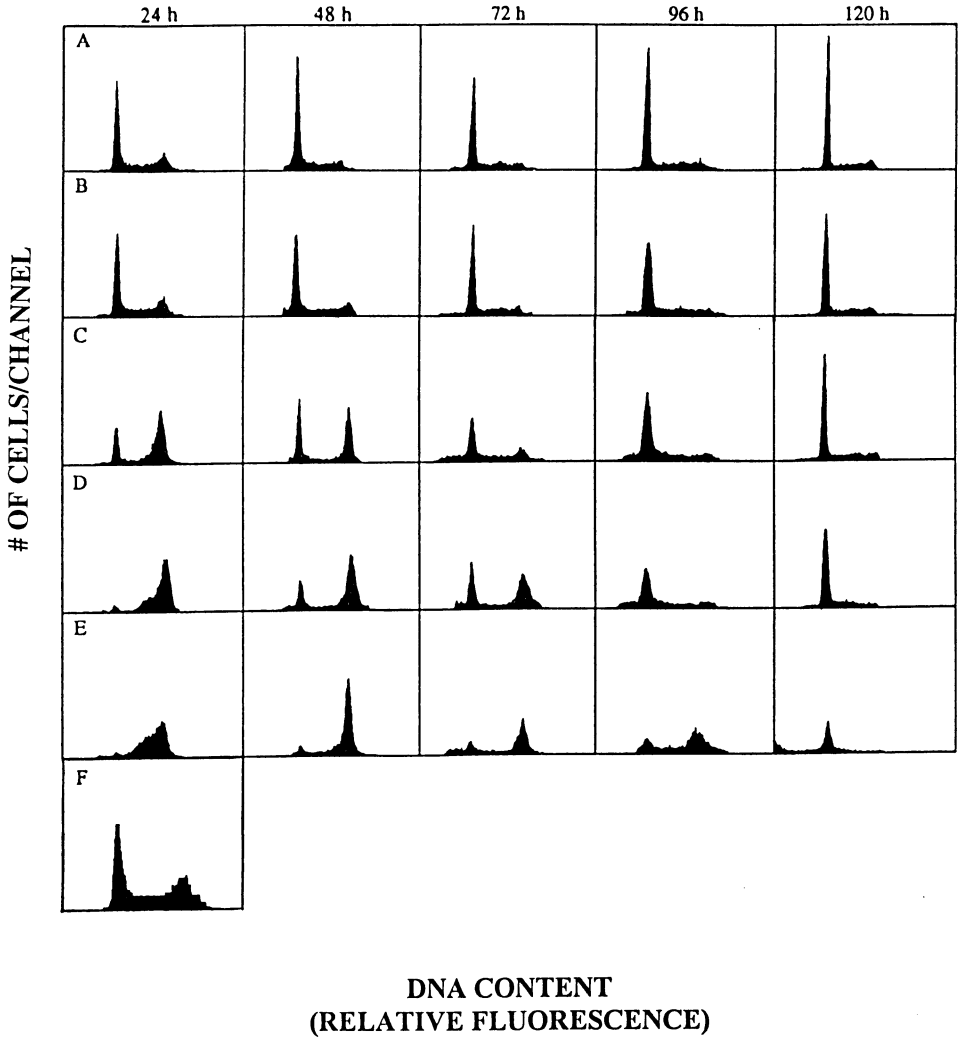

FIG. 4. DNA histograms of exponentially growing OVCAR-3 cells at various time periods after a 2-hr exposure to NIME or metabolite 7. (A) NIME, 0 μM; (B) NIME, 50 μM; (C) NIME, 100 μM; (D) NIME, 150 μM; (E) NIME, 250 μM; and (F) metabolite 7, 250 μM. Cell samples taken at different times during drug exposure were analyzed by flow cytometry. *Left peak*, G_1 cells; *right peak*, G_2M cells. S-phase cells occupy the area between the two peaks.

aqueous HCl (0.1 N) containing 0.5% Triton X-100, and kept on ice for 10 min. The acid was diluted with 5 mL of redistilled water and centrifuged at 200 *g* for 10 min. Following resuspension in 2 mL of redistilled water, the DNA was denatured by submerging the cell suspension for 10 min into a boiling water bath that was subsequently cooled in an ice slurry for 10 min. The cells were washed in PBS containing Triton X-100 (0.5%, v/v), pelleted by centrifugation, and resuspended in 100 μL of solution containing anti-BrdUrd-fluorescein (5 μg/mL) antibody and 0.1% BSA (w/v). The mixture was kept at room temperature for 30 min, and the analysis was performed on a Becton Dickinson FACScan instrument on 1–3 × 10^5 cells.

Alkaline Sucrose Density Gradient

Cells were labeled for 24 hr using a medium supplemented with 0.1 μCi/mL of [^{3}H]or [^{14}C]thymidine for internal control cells [28, 29]. Postlabeling (18–24 hr) was done before drug treatment. The drug was added for 2 hr, and the cells were allowed to grow in fresh medium for 24 hr. Then they were washed twice with PBS and dislodged by gentle scraping. To the drug-treated ^{3}H-labeled cells was added an aliquot of untreated ^{14}C-labeled cells to serve as internal control during sedimentation analysis. The cells were then lysed in the dark at 0° (lysis buffer: 0.55 N NaOH, 0.45 M NaCl, and 10 mM Na_2EDTA, 0.015% sarcosyl) and layered on the top of 5–30% sucrose gradients containing 0.3 N NaOH, 0.7 M NaCl, and 10 mM Na_2EDTA. Sedimentation was carried out at 4° in an SW41 rotor of a centrifuge, usually at 45,000 *g* overnight. Gradients were fractionated by upward displacement with 1 mL of a dye dissolved in 40% sucrose, and the samples were collected with a Bio-Rad fraction collector. The 0.3-mL fractions were analyzed by single phase liquid scintillation counting (dual-label settings).

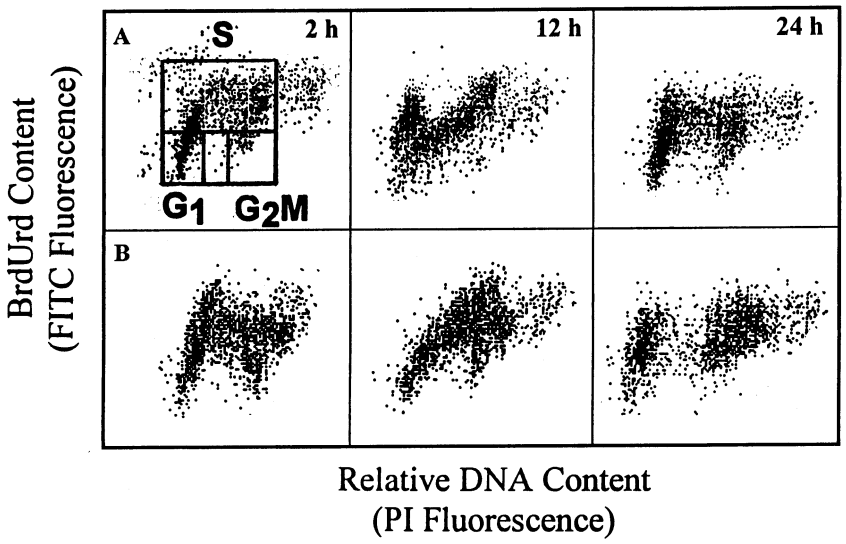

FIG. 5. Bivariate BrdUrd/PI analysis of OVCAR-3 cells. The x-axis shows the relative DNA content based on linear PI fluorescence, and the y-axis shows relative BrdUrd staining based on logarithmic FITC fluorescence. Dot plots in row A represent control untreated cells, and those representing NIME-treated cells are shown in row B.

Sequence Specificity of Guanine N^7 Alkylation

Plasmid pRGM21, which was used to determine guanine-specific N^7 alkylation, has been described in detail elsewhere [30]. Briefly, the wild-type SV40 origin of replication from the *Hin*dIII to *Sph*I site (200 bp) was inserted between the *Hin*dIII and *Sph*I sites of pBR322. Using polymerase chain reaction, the SV40 region of the plasmid was amplified with the following primers: 5′-GGCCATCCAGCCTCG-3′ and 5′-GTATCACGAGGCCCT-3′. The latter primer was end-labeled (T4 polynucleotide kinase, Gibco BRL) with [γ-^{32}P]ATP (ICN Biomedical). The amplified labeled DNA (700 bp) was exposed to temozolomide and NIME in 25 mM triethanolamine–1 mM EDTA, pH 7.2, at 37° for 2 hr. After precipitation and washing, the DNA was treated with 1 M piperidine for 15 min at 90° to produce breaks specifically at the sites of N^7 guanine alkylation. DNA fragments were separated on a 0.4 mm, 6% polyacrylamide gel in a solution containing 7 M urea and a Tris–boric acid–EDTA buffer system.

RESULTS

Survival Curves and Kinetics of Growth Reduction

Concentration–response curves from the sulforhodamine B assay demonstrated that NIME markedly inhibited the growth of OVCAR-3 cells (IC_{50} = 28 μM, 7 days post-treatment) (Fig. 1A). Almost identical levels of activity were observed under both continuous and short exposure (2 hr followed by a recovery period). The IC_{50} obtained by a 7-day clonogenic assay was 58 μM (Fig. 1B). Growth inhibition kinetics indicated a markedly delayed antiproliferative effect (147 μM, 2 days; 102 μM, 3 days; 28 μM, 7 days after treatment) (Fig. 1B). These kinetics differed from those of a pyridine-fused tetrazepinone (PYRZ) for which cytotoxic activity reached a plateau 24 hr after treatment [31].

Degradation

GC–MS analysis of the degradation products of NIME showed oxo-benzimidazole **7** at 10:40 min as the major decomposition product of NIME (Fig. 2). Its structure was confirmed by independent synthesis. A minor peak at 11:42 min corresponding to the same mass as **7** was assigned structure **8** (a structural isomer of **7**). Detailed analysis of the mass spectrometry of NIME will be reported elsewhere.

When NIME was kept at 37° for 24 hr in serum-containing medium prior to administration to tissue culture, its activity decreased markedly (Fig. 3). This excludes the possibility that metabolites of NIME may be responsible for the cytotoxic activity.

Flow Cytometry

SINGLE PARAMETER. Flow cytometry was performed on OVCAR-3 cells to determine whether incubation with NIME would induce G_2 arrest. The histograms obtained from untreated OVCAR-3 cells demonstrated a major peak (G_1) and a minor peak (G_2) (Fig. 4) (the area between these two peaks representing cells in S-phase). The histograms shown for treated OVCAR-3 cells were obtained from incubation with the drug at 50–250 μM, a range within which the drug showed a sigmoidal concentration-dependent reduction of survival. At 3 hr post-treatment, we observed late S + G_2M arrest only at the highest concentration (250 μM) (data not shown). However, 24 hr post-treatment, NIME induced a concentration-dependent accumulation of the OVCAR-3 cells in the late S + G_2M phase of the cycle. At the lowest concentrations, the arrest was transient and was reversed by 2–3 days post-treatment. At higher concentrations, the block persisted and eventually led to cell death. Also, the fraction of cells that

accumulated in S 24 hr post-treatment at supra-toxic concentrations appeared to progress through to G_2M by 2–3 days.

Metabolite **7** did not induce any significant cell cycle arrest (Fig. 4F, highest concentration).

DUAL PARAMETER. The fate of untreated OVCAR-3 S-phase cells was examined with the bi-parametric FITC-antibromodeoxyuridine/PI technique, and the results are shown in Fig. 5. The bromodeoxyuridine-positive cells (S-phase) progressed to G_2M after 12 hr; 24 hr later most of these cells had returned to G_1–S. In contrast, NIME-treated cells were still in S phase 12 hr after treatment; these S-phase cells subsequently arrested in G_2M 12 hr later. Although a small fraction of S-phase cells escaped the G_2 arrest, a negligible number of them returned to mid-S. This contrasts with control cell populations in which a significant number of cells returned to mid-S within 24 hr.

Macromolecule Synthesis

Figure 6 shows the results of incorporation of DNA and RNA precursors at 3 and 24 hr post-treatment assayed as acid-precipitable radioactivity. Concentration-dependent inhibition of DNA synthesis occurred at both time periods, the effect being less pronounced at 24 hr post-treatment. At 3 hr, protein and RNA syntheses were unaffected. At 24 hr post-treatment, a marked increase in RNA synthesis was observed. Hence, NIME appeared to selectively inhibit DNA synthesis. The inhibition of DNA synthesis was observed as early as 3 hr post-treatment, a time point at which the population distribution in late S + G_2M was minimal. These observations demonstrated that the inhibition of DNA synthesis was not a consequence of cell cycle arrest in late S + G_2M.

Alkaline Sucrose Density Gradient

To determine whether NIME induced DNA damage in OVCAR-3 cells, an alkaline sedimentation experiment was carried out at 24 hr post-treatment (a time period at which significant cell cycle perturbation was observed) (Fig. 7). At concentrations corresponding to 10–90% kill, a concentration-dependent increase in slow-sedimenting fragments was observed (Fig. 7). This indicated that NIME induced DNA damage in OVCAR-3 cells.

Sequence Specificity of Guanine N^7 Alkylation

In an attempt to define the exact damage induced by NIME, a Maxam-Gilbert sequencing assay was performed (Fig. 8). NIME at supralethal concentrations showed weak alkylating power. Despite the weakness of the bands, the experiments showed that NIME at 1 mM is capable of inducing a low level of DNA alkylation at guanine residues. However, alkylations at adenine residues were almost stronger than the corresponding guanine reactions.

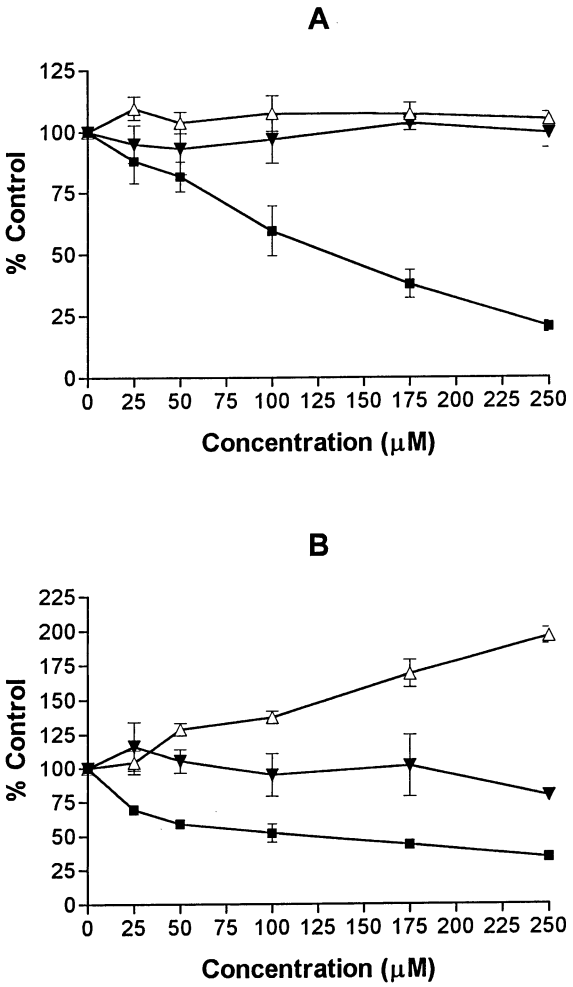

FIG. 6. Effect of NIME on macromolecule synthesis following a 2-hr drug treatment (A) 3 hr post-treatment; and (B) 24 hr post-treatment. Key: DNA (■), RNA (△), and proteins (▼). Average values for controls were 5800 cpm/10^5cells for thymidine incorporation, 4250 cpm/10^5cells for uridine, and 950 cpm/10^5cells for leucine. Points represent means ± SD of at least two separate experiments run in duplicate.

DISCUSSION

Open-chain (3-alkyl)-1,2,3-triazenes are strong alkylating agents that cause a significant degree of N^7-guanine alkylation in isolated DNA strands as determined by the Maxam-Gilbert sequencing technique [32, 33]. Temozolomide, which hydrolyzes to an open-chain triazene, produces patterns of alkylation similar to that of its triazene counterparts in this assay [32, 33]. In contrast, the tetrazepinone NIME [containing a (3-alkyl)-1,2,3-triazene moiety] shows extremely weak levels of DNA alkylation. The marked difference in alkylating capacity between NIME and temozolomide may be related to their different decomposition pathways. The major metabolite characterized from the decomposition of NIME in cell culture medium is **7**, which results from the loss of N_2 (Scheme 2). This indicates that the aqueous decomposition of NIME does not principally start with the hydrolysis of the ureido function, since this would yield a monoalkyltriazene species (**6**), as exemplified

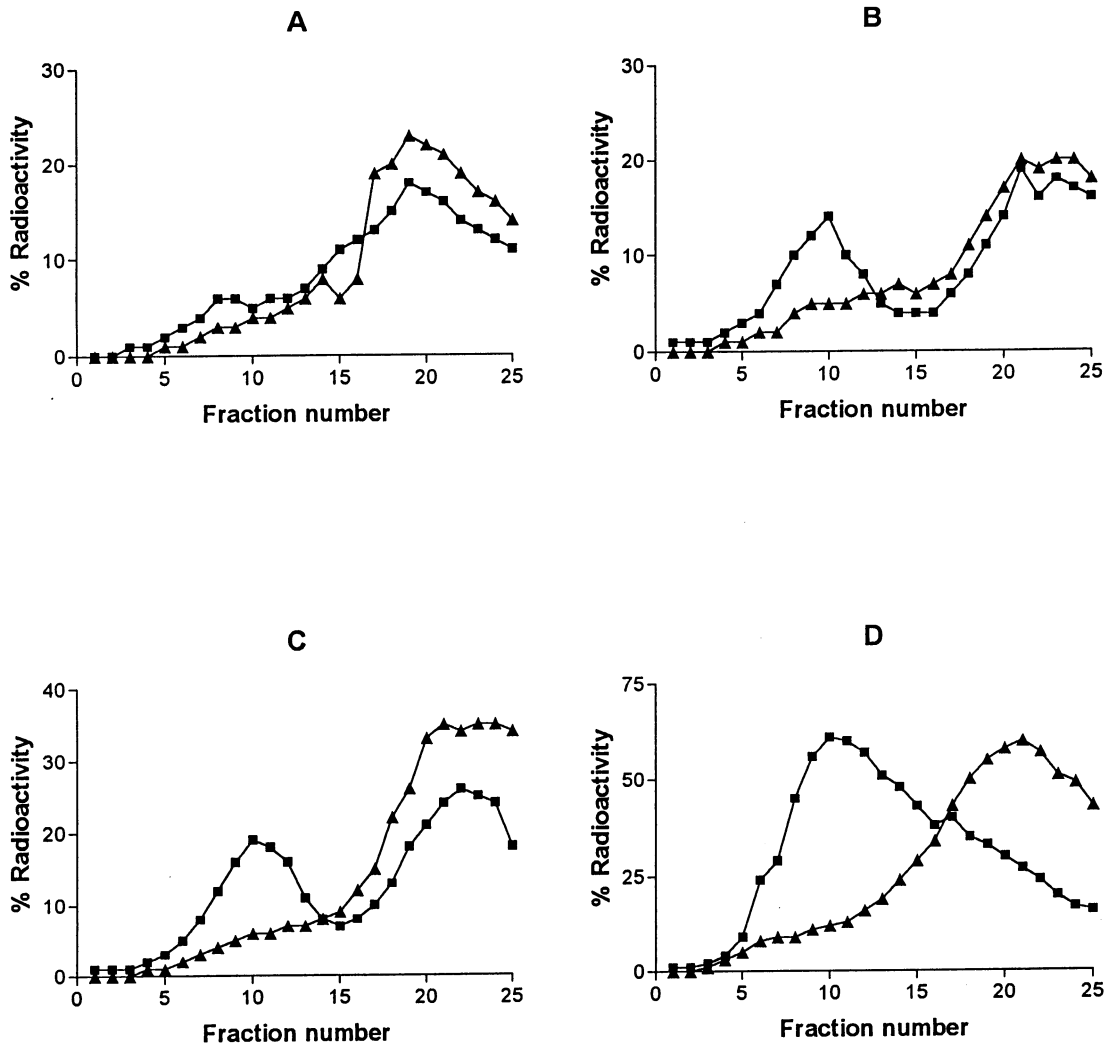

FIG. 7. DNA damage induced by NIME in OVCAR-3 cells. Key: (▲) internal control ^{14}C-labeled DNA from untreated cells, and (■) [^{3}H]thymidine-labeled DNA from treated cells. (A) 0 μM; (B) 100 μM; (C) 200 μM; and (D) 400 μM.

in Scheme 2. This marked difference in decomposition pathways between temozolomide and NIME can be explained by *ab initio* calculations, which show that the positive charge at carbonyl C-4 is higher in temozolomide (0.42) than in the tetrazepinones (0.33) [34, 35]. This is in agreement with the ureido moiety in the tetrazinone being more electrophilic and consequently more prone to hydrolysis than in the tetrazepinones.

Despite its weak alkylating power, NIME induces growth inhibition by multiple phenomena that are characteristic of cytotoxic antitumour agents (including selective inhibition of macromolecule synthesis, DNA damage, and cell cycle arrest). A concentration-dependent increase in DNA fragmentation was observed in OVCAR-3 cells at concentrations 2- to 10-fold lower than the equimolar concentration used to compare NIME with temozolomide in our Maxam-Gilbert assay. This indicates that either the drug may induce a type of DNA lesions that is not detectable by the Maxam-Gilbert assay or the drug is intracellularly converted to a DNA-reactive species. Genomic DNA damage induced by NIME was accompanied by selective inhibition of DNA synthesis and significant cell cycle arrest 24 hr after treatment (Fig. 7). We believe that the inhibition of DNA synthesis is probably caused by drug-induced DNA lesions. More importantly, while DNA synthesis was inhibited, an almost linear increase in RNA synthesis was observed in OVCAR-3 cells 24 hr after treatment. This effect may be due to the activation of transcription of many genes required to repair cellular lesions induced by the drug.

The observed effects on cell cycle progression can be explained by the interactions of NIME with DNA. At concentrations near the IC_{50}, the drug induced G_2M arrest and delayed the progress of S-phase cells through G_2M. This effect has already been associated with mechanisms that signal arrest of cell cycle progression until DNA lesions

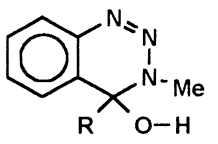

9

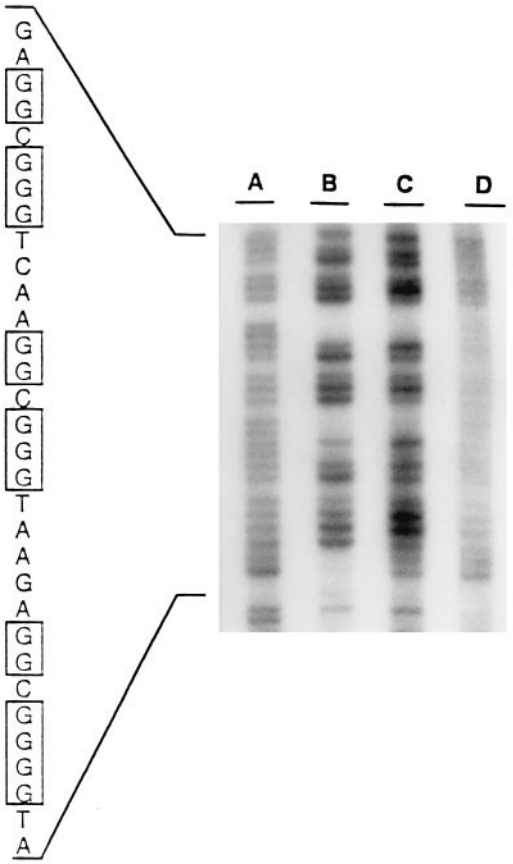

FIG. 8. Sites of N^7 alkylation produced by temozolomide and NIME at an equimolar concentration (1 mM) in the *Hin*dIII/*Sph*I sequence of SV40 DNA. Lane A, purine-specific cleavage; lane B, guanine-specific cleavage; lane C, temozolomide-treated DNA; and lane D, NIME-treated DNA. A typical guanine-rich region is indicated.

have been repaired. The observed arrests in various phases of the cell cycle, although reversible, represent a discrete cellular response to the cytotoxic lesions induced by NIME.

In summary, the weakness of the alkylating capacity of NIME and its preferred degradation pathways suggest that its cytotoxic activity may be induced by a short-lived genotoxic species (generated during its conversion to 6,5-benzofused derivatives **7** and **8**) that cannot methylate DNA bases. Furthermore, in contrast to other triazene-containing cyclic alkylating agents (e.g. benzotriazine **9** [36], imidazotetrazinones **1** [10]), the 1,2,3,5-tetrazepinone ring in NIME is prone to undergo ring contraction by losing N_2 to give 5-membered species of type **7** and **8** and, therefore, cannot be an efficient prodrug of open-chain alkyltriazene. 2-Oxobenzimidazole (**7**), the major metabolite, was 2-fold less cytotoxic than NIME (data not shown) and did not alter the cycle of OVCAR-3 cells (Fig. 4). Furthermore, when NIME was allowed to degrade in serum-containing medium prior to administration, it lost its antiproliferative activity. This indicates that its activity is due to a direct reaction of DNA bases with the drug itself or with a short-lived diazonium species as recently described [37], but not to the actions of stable metabolites **7** or **8**. Hence, considerable further work is ongoing in our laboratory to identify the precise nature of the cytotoxic lesions induced by NIME.

We thank the National Cancer Institute of Canada (NCIC) and the Barba Funds for financial support.

References

1. Carter RD, Krementz ET, Hill GJ 2nd, Metter GE, Fletcher WS, Golomb FM, Grage TB, Minton JP and Sparks FC, DTIC (NSC-45388) and combination therapy for melanoma. I. Studies with DTIC, BCNU (NSC-409962), CCNU (NSC-79037), vincristine (NSC-67574) and hydroxyurea (NSC-32065). *Cancer Treat Rep* **60:** 601–609, 1976.
2. Hill GJ 2nd, Metter GE, Krementz ET, Fletcher WS, Golomb FM, Ramirez G, Grage TB and Moss SE, DTIC and combination therapy for melanoma. II. Escalating schedules of DTIC with BCNU, CCNU, and vincristine. *Cancer Treat Rep* **63:** 1989–1992, 1979.
3. Ziegler JL, Magrath IT, Nkrumah FK, Perkins IV and Simon R, Evaluation of CCNU (NSC-79037) used for the prevention of CNS involvement in Burkitt's lymphoma. *Cancer Chemother Rep* **59:** 1155–1156, 1975.
4. Yahalom J, Voss R, Leizerowitz R, Fuks Z and Polliack A, Secondary leukemia following treatment of Hodgkin's disease: Ultrastructural and cytogenetic data in two cases with a review of the literature. *Am J Clin Pathol* **80:** 231–236, 1983.
5. Cameron LM, LaFrance RJ, Hemens CM, Vaughan K, Rajaraman R, Chubb DC and Goddard PM, Triazene metabolism. IV. Derivatives of hydroxymethyltriazenes: Potential prodrugs for the active metabolites of the anti-tumour triazene, DTIC. *Anticancer Drug Des* **1:** 27–36, 1985.
6. Kolar GF and Schlesiger J, Urinary metabolites of 3,3-dimethyl-1-phenyltriazene. *Chem Biol Interact* **14:** 301–311, 1976.
7. Manning HW, Cameron LM, LaFrance RJ, Vaughan K and Rajaraman R, Triazene metabolism. V. Chemical and biological properties of *N,N*-bis-[(1-aryl-3-methyltriazen-3-yl)-methyl]-methylamines: Potential prodrugs for the cytotoxic monomethyltriazenes. *Anticancer Drug Des* **1:** 37–43, 1985.
8. Kolar GF, Maurer M and Wildschutte M, 5-(3-Hydroxymethyl-3-methyl-1-triazeno imidazole-4-carboxamide is a metabolite of 5-(3,3-dimethyl-1-triazeno)-imidazole-4-carboxamide (DIC, DTIC NSC-45388). *Cancer Lett* **10:** 235–241, 1980.
9. Stevens MFG, Hickman JA, Stone R, Gibson NW, Baig GU, Lunt E and Newton CG, Antitumor imidazotetrazines. 1. Synthesis and chemistry of 8-carbamoyl-3-(2-chloroethyl)imidazo[5,1-*d*]-1,2,3,5-tetrazin-4(3*H*)-one, a novel broad-spectrum antitumor agent. *J Med Chem* **27:** 196–201, 1984.
10. Baig GU and Stevens MFG, Antitumor imidazotetrazines. Part 12. Reactions of mitozolomide and its 3-alkyl congeners with oxygen, nitrogen, halogen, and carbon nucleophiles. *J Chem Soc Perkin Trans 1*: 665–667, 1987.
11. Newlands ES, Blackledge G, Slack JA, Goddard C, Brindley CJ, Holden L and Stevens MFG, Phase I clinical trial of mitozolomide. *Cancer Treat Rep* **69:** 801–805, 1985.
12. Newlands ES, Blackledge GRP, Slack JA, Rustin GJS, Smith DB, Stuart NSA, Quarterman CP, Hoffman R, Stevens MFG, Brampton MH and Gibson AC, Phase I trial of temozolomide (CCRG 81045: M&B 39831: NSC 362856). *Br J Cancer* **65:** 287–291, 1992.
13. O'Reilly SM, Newlands ES, Glaser MG, Brampton M, Rice-Edwards JM, Illingworth RD, Richards PG, Kennard C, Colquhoun IR, Lewis P and Stevens MFG, Temozolomide: A new oral cytotoxic chemotherapeutic agent with promising

activity against primary brain tumours. *Eur J Cancer* **29A:** 940–942, 1993.
14. Baer JC, Freeman AA, Newlands ES, Watson AJ, Rafferty JA and Margison GP, Depletion of O^6-alkylguanine-DNA alkyltransferase correlates with potentiation of temozolomide and CCNU toxicity in human tumour cells. *Br J Cancer* **67:** 1299–1302, 1993.
15. Mitchell RB and Dolan ME, Effect of temozolomide and dacarbazine on O^6-alkylguanine-DNA alkyltransferase activity and sensitivity of human tumor cells and xenografts to 1,3-bis(2-chloroethyl)-1-nitrosourea. *Cancer Chemother Pharmacol* **32:** 59–63, 1993.
16. Bull VL and Tisdale MJ, Antitumor imidazotetrazines—XVI: Macromolecular alkylation by 3-substituted imidazotetrazinones. *Biochem Pharmacol* **36:** 3215–3220, 1987.
17. Jean-Claude BJ and Just G, Synthesis of bi- and tricyclic tetrazepinones. *J Chem Soc Perkin Trans 1*: 2525–2529, 1991.
18. Jean-Claude BJ, Synthesis and spectral studies of tetrazepinones. *Ph.D. Dissertation*, pp. 50–123. McGill University, Montreal, 1992.
19. Jean-Claude BJ, Damian S, Damian Z, Do Khan L, Chan TH and Leyland-Jones B, Tetrazepinones: A new class of DNA-directed antitumor agents. *Proc Am Assoc Cancer Res* **35:** 402, 1994.
20. Jean-Claude BJ, Mustafa A, Damian Z, De Marte J, Chan TH and Leyland-Jones B, Comparative studies on the action of Temozolomide and two novel tetrazepinones on OVCAR-3 cell line *in vitro*. *Proc Am Assoc Cancer Res* **36:** 349, 1995.
21. Jean-Claude BJ, Mustafa A, Damian Z, De Marte J, Vasilescu DE, Yen R, Chan TH and Leyland-Jones B, Comparative studies between the effects of mitozolomide and two novel tetrazepinones PYRCL and QUINCL on NIH:OVCAR-3 cells. *Cancer Chemother Pharmacol* **42:** 59–67, 1998.
22. Jean-Claude BJ, Mustafa A, Watson AJ, Damian Z, Vasilescu D, Chan TH and Leyland-Jones B, The tetrazepinones are equally cytotoxic to Mer^+ and Mer^- human tumour cell lines. *J Pharmacol Exp Ther*, in press.
23. Jean-Claude BJ and Just G, Synthesis and stability of 5-, 7- and 8-substituted benzo-1,2,3,5-tetrazepin-4-ones. *Heterocycles* **48:** 1347–1364, 1998.
24. Hamilton TA, Young TC, McKoy RC, Grotzinger WM, Green KR, Chu JA, Whang-Peng EW, Rogan J, Green AM and Ozols WR, Characterization of a human ovarian carcinoma cell line (NIH: OVCAR-3) with androgen and estrogen receptors. *Cancer Res* **43:** 5379–5389, 1983.
25. Skehan P, Storeng R, Scudiero D, Monks A, McMahon J, Vistica D, Warren JT, Bokesch H, Kenney S and Boyd MR, New colorimetric cytotoxicity assay for anti-cancer drug screening. *J Natl Cancer Inst* **82:** 1107–1112, 1990.
26. Clark SA, Stevens MFG, Sansom CE and Schwalbe CH, Antitumour imidazotetrazines, mitozolomide and Temozolomide. Probes for the major groove of DNA. *Anticancer Drug Des* **6:** 63–68, 1990.
27. Dolbeare F, Gratzner H, Pallavacini MG and Gray JW, Flow cytometric measurement of total DNA content and incorporated bromodeoxyuridine. *Proc Natl Acad Sci USA* **80:** 5573–5577, 1983.
28. Pera MF Jr, Rawlings CJ, Shackleton J and Roberts JJ, Quantitative aspects of the formation and loss of DNA interstrand crosslinks in Chinese hamster cells following treatment with *cis*-diamminedichloroplatinum(II) (cisplatin). II. Comparison of results from alkaline elution, DNA renaturation and DNA sedimentation studies. *Biochim Biophys Acta* **655:** 152–166, 1981.
29. Plowman J, Waud WR, Koutsoukos AD, Rubinstein LV, Moore TD and Grever MR, Preclinical antitumor activity of temozolomide in mice: Efficacy against human brain tumor xenografts and synergism with 1,3-bis(2-chloroethy1)-1-nitrosourea. *Cancer Res* **54:** 3793–3799, 1994.
30. Nobile C and Martin RG, Stable stem-loop and cruciform DNA structures: Isolation of mutants with rearrangements of the palindromic sequence at the simian virus 40 replication origin. *Intervirology* **25:** 158–171, 1986.
31. Jean-Claude BJ, Mustafa A, Damian Z, De Marte J, Yen R, Chan TH and Leyland-Jones B, Design and mechanism of action of a novel cytotoxic 1,2,3-triazene-containing heterocycle, 3,5-dimethyl-pyrido-1,2,3,5-tetrazepin-4-one (PYRZ), in the human epithelial ovarian cancer cell line NIH: OVCAR-3 *in vitro*. *Br J Cancer* **76:** 467–473, 1997.
32. Hartley JA, Mattes WB, Vaughan K and Gibson NW, DNA sequence specificity of guanine N^7-alkylations for a series of structurally related triazenes. *Carcinogenesis* **9:** 669–674, 1988.
33. Hartley JA, Gibson NW, Kohn KW and Mattes WB, DNA sequence selectivity of guanine-N7 alkylation by three antitumor chloroethylating agents. *Cancer Res* **46:** 1943–1947, 1986.
34. Williams CI, Whitehead MA and Jean-Claude BJ, Equilibrium geometries and enantiomeric interconversions in tetrazepinone ring systems: A semi-empirical and *ab initio* treatment. *Theochem—J Mol Struct* **392:** 27–42, 1997.
35. Williams CI, Whitehead MA and Jean-Claude BJ, A semi-empirical PM3 treatment of benzotetrazepinone decomposition in acid media. *J Org Chem* **62:** 7006–7014, 1997.
36. LaFrance RJ, Manning HW and Vaughan K, Open-chain nitrogen compounds. Part XII. Methanolysis of 3-alkyl-3,4-dihydro-1,2,3-benzotriazin-4-ols: Evidence for ring-chain tautomerism with the cytotoxic monoalkyltriazenes. *Can J Chem* **65:** 292–297, 1987.
37. Jean-Claude BJ and Williams CI, ^{15}N NMR studies of bi- and tricyclic tetrazepinones. *Magn Res Chem* **36:** 87–91, 1998.